nature protocols

PROTOCOL

https://doi.org/10.1038/s41596-022-00782-8

In situ electrochemical Raman spectroscopy and ab initio molecular dynamics study of interfacial water on a single-crystal surface

Yao-Hui Wang[1,6], Shunning Li[2,6], Ru-Yu Zhou[1], Shisheng Zheng[2], Yue-Jiao Zhang[1,3], Jin-Chao Dong[1,3], Zhi-Lin Yang[1], Feng Pan[2]✉, Zhong-Qun Tian[1,3] and Jian-Feng Li[1,3,4,5]✉

The dynamics and chemistry of interfacial water are essential components of electrocatalysis because the decomposition and formation of water molecules could dictate the protonation and deprotonation processes on the catalyst surface. However, it is notoriously difficult to probe interfacial water owing to its location between two condensed phases, as well as the presence of external bias potentials and electrochemically induced reaction intermediates. An atomically flat single-crystal surface could offer an attractive platform to resolve the internal structure of interfacial water if advanced characterization tools are developed. To this end, here we report a protocol based on the combination of in situ Raman spectroscopy and ab initio molecular dynamics (AIMD) simulations to unravel the directional molecular features of interfacial water. We present the procedures to prepare single-crystal electrodes, construct a Raman enhancement mode with shell-isolated nanoparticle, remove impurities, eliminate the perturbation from bulk water and dislodge the hydrogen bubbles during in situ electrochemical Raman experiments. The combination of the spectroscopic measurements with AIMD simulation results provides a roadmap to decipher the potential-dependent molecular orientation of water at the interface. We have prepared a detailed guideline for the application of combined in situ Raman and AIMD techniques; this procedure may take a few minutes to several days to generate results and is applicable to a variety of disciplines ranging from surface science to energy storage to biology.

Introduction

Electrocatalysis at the electrode/electrolyte interface that can efficiently convert water, carbon dioxide and nitrogen molecules in the air into higher-value products, is one of the key techniques for sustainable energy[1–6]. The structure of interface, known as the electric double layer (EDL), is widely believed to play an essential role in electrocatalysis[7–9]. In aqueous systems, water molecules are the major components of the interfacial EDL and direct participants in electrocatalysis processes, such as hydrogen evolution/oxidation reactions[10,11], oxygen reduction/evolution reactions[12–14] and carbon dioxide/nitrogen reduction reactions[15–18]. Single-crystal electrodes possess well-defined surface structures and electric field distributions; thus, importantly, they can be well modeled at the atomic level for elucidating electrocatalytic reaction mechanisms[19–21]. Therefore, dynamic processes associated with interfacial water on an atomically flat single-crystal surface can provide a platform for understanding electrocatalysis[22]. However, acquiring information of interfacial water in the EDL during electrocatalysis processes remains elusive on the atomically flat single-crystal surfaces, owing to the complexity of interfacial reaction processes, significant signal perturbation from bulk water and lack of practical surface characterization techniques.

There is a growing number of in situ characterization techniques that are being used to probe interfacial water, such as surface-enhanced infrared absorption spectroscopy[23,24], sum-frequency generation spectroscopy[25–27] and x-ray spectroscopy[7,28]. However, most of these techniques only provide information about interfacial water close to the potential of zero charge (PZC) where the excess electronic charge density of a metal–solution interface is zero. However, a number of

[1]College of Materials, State Key Laboratory of Physical Chemistry of Solid Surfaces, MOE Key Laboratory of Spectrochemical Analysis and Instrumentation, iChEM, College of Chemistry and Chemical Engineering, College of Energy, College of Physical Science and Technology, Xiamen University, Xiamen, China. [2]School of Advanced Materials, Peking University, Shenzhen Graduate School, Shenzhen, China. [3]Innovation Laboratory for Sciences and Technologies of Energy Materials of Fujian Province (IKKEM), Xiamen, China. [4]College of Optical and Electronic Technology, China Jiliang University, Hangzhou, China. [5]Shenzhen Research Institute of Xiamen University, Shenzhen, China. [6]These authors contributed equally: Yao-Hui Wang, Shunning Li. ✉e-mail: panfeng@pkusz.edu.cn; li@xmu.edu.cn

important electrocatalysis processes tend to occur at a potential that is much higher or much lower than the PZC[29,30]. Thus, details about the structure and composition of interfacial water at extreme electrocatalytic potentials are lacking, which limits the comprehensive understanding of electrocatalysis.

SERS for the study of interfacial water

Highly sensitive surface-enhanced Raman spectroscopy (SERS) methods are capable of single-molecular-level resolution[31,32], which makes them well suited for the detection of interfacial water. In addition, the Raman signal of water is very weak in conventional Raman spectroscopy owing to the tiny Raman scattering cross-section of water molecules. Unlike infrared spectroscopy, which will be seriously interfered by bulk water, SERS can easily eliminate the interference from signals of bulk water when probing the interfacial water, because only water signals close to the surface are enhanced. Moreover, SERS possesses a wider spectral detection range than infrared spectroscopy, especially in the low wavenumber range (down to ~2 cm^{-1}) (refs. [33,34]), which provides a wealth of information about the hydrogen bond, structure and composition of interfacial water. In this context, SERS is an appropriate technique to study interfacial water.

Since the discovery of SERS in 1977, scientists have begun to use SERS to study interfacial water. In 1981, Fleischmann et al.[35] obtained the SERS spectra of interfacial water for the first time and provided fruitful information of interfacial water in H-O-H bending and O-H stretching vibration. At that time, it was necessary to add a large amount of halide ions to improve the enhancement effect for the study of interfacial water by SERS. In 1987, Funtikov et al.[36] obtained the SERS spectra of interfacial water in a system without coadsorbed ions, but only the H-O-H bending vibration information of water was provided. In 1990, Tian's groups[37–39] obtained the clear SERS spectra of interfacial water on Au, Ag and Cu surfaces by improving the method of SERS enhancement, which extended the SERS study of interfacial water to nonhalogen systems. The H-O-H bending vibration peaks and O-H stretching vibration peaks of interfacial water on Au, Ag and Cu surfaces were significantly enhanced. However, information on interfacial water on transition metal surfaces is of utmost interest to electrochemists, but is still poorly understood. From 2007 to 2010, Jiang and Li et al. used a 'borrowing' strategy to construct core-shell nanoparticles (NPs) (Au as inner core and transition metal as shell) to study the behavior of interfacial water on transition metal (Pt, Pd, Rh, etc.) surfaces[40,41]. The inner Au can enhance the Raman signals generated by interfacial water on transition metal surfaces because the interfacial water locates in the range of enhancement. Unfortunately, all of the above studies are on the surface of polycrystalline electrodes. SERS study of interfacial water on the atomically flat single-crystal surface is indispensable for the rationalization of interfacial reaction processes and reaction mechanisms.

However, SERS cannot be directly used to probe interfacial water on a single-crystal surface because atomically flat surfaces fail to meet the SERS requirement of a surface plasmon resonance effect. The development of the shell-isolated nanoparticle-enhanced Raman spectroscopy (SHINERS)[42] technique successfully overcame this intrinsic morphological limitation of SERS. SHINERS utilizes the strong coupling effect of inner Au of shell-isolated NPs (SHINs) with pure Au, Ag and Cu electrodes to enhance the Raman signals on a single-crystal surface, has extremely high surface sensitivity and can effectively probe interfacial water on a single-crystal surface.

In the previous work published by our research group, Li et al. used SHINERS to study the interfacial water on low-index Au single-crystal surfaces, and clearly revealed the dynamic structural variation of interfacial water at bias potentials[43]. We (Wang et al.) then studied the structure and dissociation of interfacial water on a Pd single-crystal surface by combining SHINERS and ab initio molecular dynamics (AIMD)[44]. According to these results, interfacial water displays different water structures and composition on a Pd single-crystal surface, composed of hydrogen-bonded water and cation-hydrated water. Under bias potential, the coordinating water molecules around cations move toward the Pd surface, which reduces the effective distance between Pd and protons from $M.H_2O$, thus improving their charge transfer efficiency and enhancing the hydrogen evolution reaction (HER) performance. In terms of thermodynamics, through local hydrated cation tuning strategies around the interface, disordered bulk H_2O can be effectively arranged into ordered interfacial H_2O (i.e., an entropy decrease process) in a finite region to minimize additional work done and to maximize electrochemical energy conversion. In this regard, by altering the transmission route of H_2O, interfacial cations serve as a 'co-catalyst' at the interface by continuously supplying water to the surface and transferring the hydroxyl radical to solution during water dissociation.

In the analysis of spectroscopic results from SHINERS, AIMD simulation could aid in the atomic understanding of the orientational configurations of interfacial water. AIMD simulation is renowned for its capability in modeling the structure and dynamics of materials at the atomistic scale. In this method, the motion of nuclei is numerically determined by solving Newton's equations in an identical framework to the traditional force-field molecular dynamics (MD) simulation, while the forces on the nuclei at each AIMD step are derived from an electronic structure calculation within density functional theory[45]. Compared with the force-field approach, AIMD is free of ad hoc parametrizations and can explicitly take into account the polarization of electrons, making it especially powerful for the interpretation of experimental observations in the realm of catalysis in aqueous media[46,47].

Many pioneering studies have utilized AIMD simulation to gain illuminating insights into both the transport behavior of ions in aqueous solutions and the structural evolution in the interfacial region. For example, Tuckerman et al. performed AIMD simulations to investigate the solvated state of proton in water, and justified the existence of Eigen and Zundel cations that shows the ordering of local structure of water molecules[48]. Galli et al. combined AIMD and many-body perturbation theory calculations to analyze the effect of surface water on the band structure of functionalized Si[49]. Selloni et al. revealed the dynamics of excess electron at the aqueous interface of TiO_2 and demonstrated the facet-dependent catalytic behavior that is in good agreement with experimental observations[47]. These studies not only complimented previous experimental findings, but also motivated new experimental works. We therefore speculate that the combinatorial application of SHINERS measurement and AIMD simulation, as employed in recent works to probe the microscopic structure of interfacial water[44], could serve as a promising route to unravel the electrocatalytic processes and can be adopted by researchers from a variety of related disciplines.

Limitations

Limitations of this in situ Raman study of interfacial water relate to the fact that the measurement devices need to be added to the system being analyzed. The conditions at the interface might, therefore, not be exactly the same as they would be if they were not being measured.

Changes introduced by the analytical conditions include:

- The necessary use of a negative potential on the electrode surface that is being analyzed
- The inhomogeneity of enhancement effect at each sampling point
- The disturbances resulting from the Raman amplifier (i.e., artifacts such as an electromagnetic field, SiO_2 shell and impurities that are introduced when adding the SHINs)

The limitations of AIMD mainly include the huge computational costs, the coupling of electrode potential and cation concentration, the short simulation time (10–100 ps) and the small simulation cell (100–200 atoms).

Overview of the procedure

Procedures for the study of interfacial water on a single-crystal surface using in situ electrochemical Raman and AIMD are included in Fig. 1. Au single crystal is our target substrate. SHINs are the amplifier of Raman signal. Preparation and characterization of Au single crystals and SHINs are the first step, then carrying out in situ Raman to obtain the spectra of interfacial water. Finally, the AIMD is used to simulate the variation of interfacial water under electric field.

Characterization

It is particularly important to test whether there are any pinholes in the SiO_2 shell of SHINs. An insufficiently dense SiO_2 shell with abundant pinholes allows molecules in the external environment to adsorb on the core Au surface. If the SHINs have pinholes, the signal generated by the adsorption of water on the inner Au surface rather than the target substrate, will seriously affect the experimental outcome. Pyridine is a good choice of reagent for testing for pinholes because it attaches specifically to the inner Au surface, but does not interact with the SiO_2 shell. If there are any pinholes, these will be evident from the presence of pyridine peaks in the Raman spectrum.

Pyridine is also the reagent of choice for determining the surface enhancement factor (EF)—a widely accepted parameter for quantitative evaluation of SERS performance. If the enhancement effect of SHINs is poor, the Raman signals of interfacial water will be hard to obtain owing to the

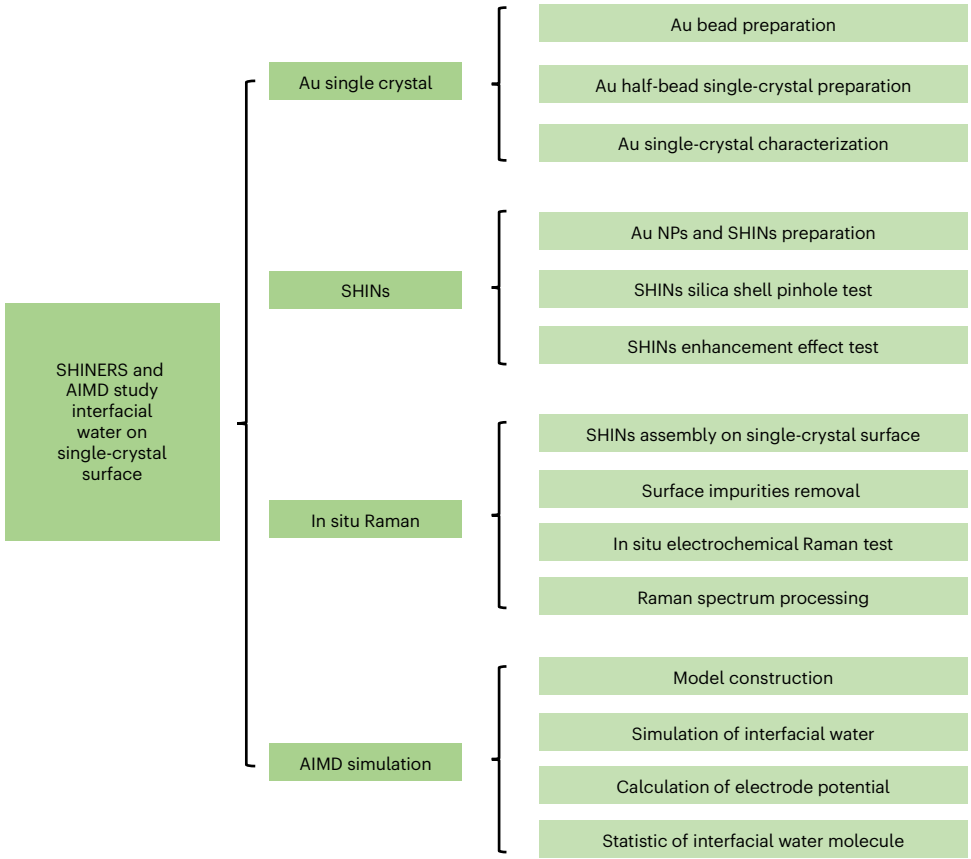

Fig. 1 | Schematic representation. Combined SHINERS and AIMD study of interfacial water on a single-crystal surface. The procedure is divided into four sections.

interference from bulk water. Therefore, the shells of SHINs must be extremely thin and dense without pinholes to support a high enhancement effect and to isolate the interference.

Materials

Reagents

- Milli-Q water (18.2 MΩ cm, 25 °C)
- Hydrochloric acid, HCl (analytical reagent (AR), 36.0–38.0%, Sinopharm Chemical Reagent, CAS no. 7647-01-0)
- Nitric acid, HNO_3 (AR, 65.0–68.0%, Sinopharm Chemical Reagent, CAS no. 7697-37-2)
- Methylene chloride, CH_2Cl_2 (AR, 99.5%, Sinopharm Chemical Reagent, CAS no. 75-09-2)
- Hydrogen peroxide, H_2O_2 (AR, 30%, Sinopharm Chemical Reagent, CAS no. 7722-84-1)
- Sulfuric acid, H_2SO_4 (96%, Merck KGaA, CAS no. 7664-93-9)
- Trisodium citrate dihydrate, $Na_3C_6H_5O_7{\cdot}2H_2O$ (99.0%, Alfa Aesar, CAS no. 6132-04-3)
- Hydrogen tetrachloroaurate(III) trihydrate, $HAuCl_4{\cdot}3H_2O$ (99.99%, Alfa Aesar, CAS no. 16961-25-4)
- (3-Aminopropyl) trimethoxysilane, APTMS (97%, $\rho = 1.027$ g mL^{-1} at 25 °C, Alfa Aesar, CAS no. 13822-56-5)
- Sodium silicate solution, $Na_2O(SiO_2)_x{\cdot}xH_2O$ (~10.6% Na_2O and ~26.5% SiO_2, $\rho = 1.39$ g mL^{-1} at 25 °C, Sigma-Aldrich, Product number: 338443)
- Sodium hydroxide, NaOH (99.99%, Alfa Aesar, CAS no. 1310-73-2)
- Pyridine, C_5H_5N (>99.5%, Alfa Aesar, CAS no. 110-86-1)
- Sodium perchlorate, $NaClO_4$ (98.0–102.0%, Alfa Aesar, CAS no. 7601-89-0)
- 2-part Epoxy/2K Epoxy (Loctite, Double Bubble)
- De-alumina powder (99.9%, 1.0/0.3/0.05 μm, Qmaxis)
- Hydrogen gas, H_2 (99.999%, Linde)

- Oxygen gas, O_2 (99.999%, Linde)
- Argon gas, Ar (99.999%, Linde)

Equipment

- Beaker
- Round-bottom flask
- Quartz coverslip
- Sandpaper
- Polishing cloth
- N-Si(111) wafer, 525 ± 25 μm thickness, Si wafer cut into 0.5 × 0.5 cm^2 square before use
- Au wafer: 100 nm thickness of Au films were deposited on Si(111) wafer at a rate of 2 Å s^{-1} by E-beam evaporation to obtain Au wafer
- Au wire, 0.5 mm diameter (purity 99.99%, Sigma-Aldrich, CAS no. 7440-57-5)
- Pt wire, 0.5 mm diameter (purity 99.99%, Sigma-Aldrich, CAS no. 7440-06-4)
- Homemade reversible hydrogen electrode (RHE); see 'Equipment setup'
- Homemade electrochemical glass cell; see 'Equipment setup'
- Homemade Teflon Raman cell; see 'Equipment Setup'
- CHI 760E electrochemical workstation (CH Instruments)
- Potentiostat (Autolab PGSTAT30, Metrohm)
- Confocal microscope Raman system XploRA (HORIBA, France)
- High-resolution transmission electron microscope JEM-2100 (JEOL, Japan)

Reagent setup

Chloroauric acid (0.86% (wt/vol))

1.0 g of hydrogen tetrachloroaurate(III) trihydrate (solid) was dissolved into 100 mL of Milli-Q water in a volumetric flask (100 mL). Store this solution at room temperature (25 °C) for at least 2 d before use.

APTMS solution (1 mM)

18.0 μL of APTMS was diluted into 100 mL of Milli-Q water in a volumetric flask (100 mL). The final concentration of APTMS is 1.0 mM. This solution is prepared before use.

Sodium silicate solution (0.54%, wt/wt)

2.0 mL of sodium silicate solution (27%, wt/wt) was added in a volumetric flask (100 mL) and then 92 mL of Milli-Q wate was added. Add 6 mL of hydrochloric acid solution (0.1 M) to the flask with fast shaking to adjust the pH. The concentration of sodium silicate is 0.54% (wt/wt), and the pH is ~10. This solution is prepared before use.

Equipment setup

Homemade RHE

In the RHE, H_2 is generated electrochemically from the reduction of H^+ in the electrolyte used in the experiment. The RHE was transferred to fresh electrolyte for 30 min before use. The potential calibration of RHE was made by verifying the position of hydrogen adsorption/desorption peaks of Pt(111) in 0.1 M $HClO_4$ with the standard cyclic voltammetry (CV) of Pt(111).

Electrochemical cell

A homemade three-compartment glass cell, with a Pt wire and a homemade RHE as the counter and the reference electrodes, respectively, was used for electrochemical measurements. The three-compartment glass cell can separate the reactions occurring at working and counting electrode surfaces, and decrease the influence from the reference electrode if using a non-RHE as the reference electrode. The electrochemical cell is thoroughly cleaned by soaking in concentrated sulfuric acid for 12 h before use.

Raman cell

A homemade Teflon Raman cell, with a Pt wire and a homemade RHE as the counter and the reference electrodes, respectively, was used for the in situ electrochemical Raman measurements. As with electrochemical cell cleaning, the Raman cell is thoroughly cleaned before use by soaking in

concentrated sulfuric acid for 12 h. Long-time Raman tests should use an Au wire to replace the Pt wire as the counting electrode, avoiding Pt deposition on Au working electrode surface.

Raman instrument

A He-Ne laser with 637.8 nm excitation wavelength and a 50× microscope objective with a numerical aperture of 0.55 were used in all measurements. Raman frequencies were calibrated by a Si wafer during each experiment.

Procedure

Section 1: preparation of an Au single crystal

Preparation of Au bead ● Timing 2 h

▲ CRITICAL In this process, the primary objective is to prepare the Au bead with a perfect crystal structure.

1 Melt the end of Au wire with a diameter of 0.5 mm and length of at least 5 cm into a bead of 2 mm in diameter by a hydrogen flame.
   ! CAUTION Wear anti-glare sunglasses to protect your eyes before melting.
2 Immerse the molten state of the Au bead in the aqua regia (the ratio of HCl/HNO_3 volume is 3:1) to remove the impurities.
   ▲ CRITICAL STEP The impurities are often visible and can be seen as bright flecks shining at the molten state of the bead surface.
   ! CAUTION The aqua regia is quite dangerous; ensure that you do not splash it.
3 Melt the bead again to check for impurities after cleaning the residual aqua regia.
4 Repeat Steps 2 and 3 until the bead is free of impurities.
5 After impurities have been removed, keep the molten state of the half-bead under hydrogen flame for ~60 s and cool the bead very slowly by moving it up and down the hydrogen flame from the joint of the bead and wire to the end of the bead.
6 Select the bead with symmetrically dispersed (111) and (100) facets to mechanically polish.

Preparation of Au half-bead single crystal ● Timing 2–3 d

▲ CRITICAL Clavilier-type Au(111), Au(100) and Au(110) half-bead single crystals were prepared in this work.

7 Select the target facet of the Au bead by the laser positioning method on the single-crystal polisher machine. Fix the facet in a specific direction with epoxy.
8 Polish the bead to two-thirds the size with sandpaper, following the order of 800 mesh to 1,200 mesh to 2,400 mesh to 4,800 mesh. At this time, we can see a very bright hemispherical surface with the naked eye.
   ▲ CRITICAL STEP If the hemispherical surface is not bright or scratches are still visible after Step 8, repeat the sandpaper grinding until the hemispherical surface is bright.
9 Replace sandpaper with a polishing cloth, and polish the two-thirds bead to a brighter mirror with a polishing solution of 1 μm (1 h), 0.3 μm (1 h) and 0.05 μm (1–2 h). The two-thirds bead was polished to a half bead.
10 Carefully take down the half bead, which is fixed in the epoxy, and remove the epoxy using methylene chloride.
   ! CAUTION Pay attention to personal protection when using methylene chloride. Respiratory system protection: wear a gas mask or half mask. Eye protection: wear chemical safety goggles. Body protection: wear protective clothing. Hand protection: wear chemical-resistant gloves.
11 Remove surface organic substances by soaking in piranha solution for 12 h.
   ! CAUTION Preparation of piranha solution requires wearing rubber gloves and appropriate facial protection in a fume cupboard. Slowly add hydrogen peroxide to sulfuric acid solution in a beaker. This process gives off a lot of heat. It is important to be patient and to perform the addition in this order; it is dangerous to add sulfuric acid to hydrogen peroxide.
12 Electropolish the half-bead in 0.5 M H_2SO_4 solution at 5.0 V for 10–15 s (using a clean Au wire as counting electrode). Remove the residual H_2SO_4 with ultrapure water. Then, immerse the half-bead in 0.5 M HCl solution for 1 min to remove the surface oxidation layer. Remove the residual HCl with ultrapure water. Repeat three times.
13 Anneal the half-bead in a tubular furnace at 800 °C for 12 h under an H_2–Ar mixed atmosphere (5% H_2, 95% Ar).

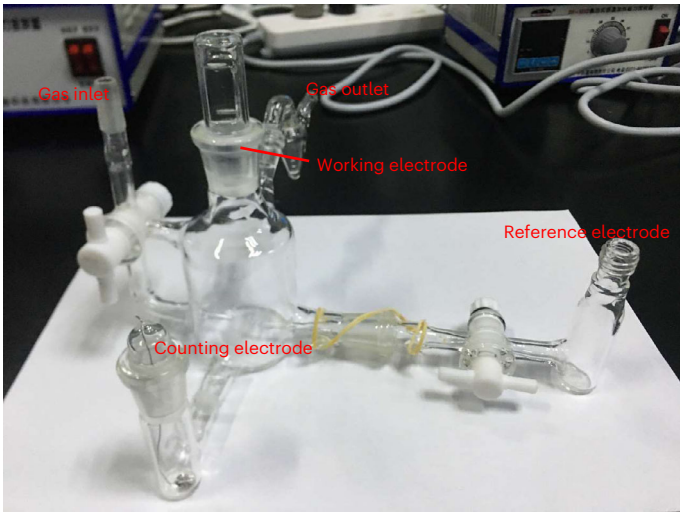

Fig. 2 | Equipment setup. Electrochemical glass cell for single-crystal CV test.

Characterization of Au single crystals by CV ● Timing 1 h

▲ **CRITICAL** Electrochemical CV is used to characterize the quality of Au single crystals.

14 Prepare fresh 60 mL, 0.05 M H_2SO_4 solution in an electrochemical glass cell (Fig. 2).

15 Anneal the Au single crystal with a butane flame.

▲ **CRITICAL STEP** Quickly transfer the crystal into a glass container with pure water under an Ar stream and cool down to ambient temperature.

16 Drop pure water to protect the annealed Au single crystal and transfer the clean Au single crystal to the prepared electrochemical glass cell.

17 Bring the Au single crystal into contact with the electrolyte in a hanging meniscus configuration (Fig. 3a) under the potential where no electrochemical reaction takes place.

▲ **CRITICAL STEP** A hanging meniscus configuration ensures that only the target facet participates in electrochemical reaction.

18 Select an Au(111) single crystal as the sample to collect the CV of Au(111) in 0.05 M H_2SO_4 with a 10 mV s^{-1} scan rate.

19 Check that the CV (Fig. 3b) of Au(111) shows the standard features, including surface reconstruction and lifting peak (~0.58 V), sulfate adsorption/desorption peak (~0.75 V) and ordered sulfate phase transformation peak (~1.06 V). If the peak height of sulfate phase transformation peak is equal to or greater than the surface reconstruction and lifting peak in the CV of Au(111), this indicates that the quality of the Au(111) is good.

Section 2: preparation and characterization of SHINs

Preparation of Au NPs and SHINs

20 Prepare 55 nm Au nanospheres as described[50]. In our lab, the steps are as follows:
- Boil 200 mL of $HAuCl_4$ solution (0.01% wt/vol); in our lab the solution is heated using a thermocouple
- Quickly add 1.4 mL of sodium citrate solution (1%, wt/vol) into the boiling solution
- Maintain boiling with reflux for 30 min
- Allow the solution to cool naturally to ambient conditions of ~25 °C

21 Synthesize the SHINs as described in the literature[42]; in our lab the steps are as follows:
- Add 0.4 mL of APTMS solution (1 mM) to 30 mL of undiluted 55 nm Au nanosphere solution
- Add 3.2 mL of sodium silicate solution (0.54% wt/wt) with a pH of ~10 to the mixture
- Transfer the solution to a 99 °C water bath and stir for ~20 min to coat the SiO_2 shell
- Take 2.0 mL as-prepared SHINs solution to centrifuge in a 2.0 mL centrifuge tube at 2,000*g* for 10 min (at room temperature). Remove the supernatant and wash the SHINs with 2.0 mL ultrapure water, centrifuging with the same conditions and removing the supernatant. Obtain the bottom residue
- Add 0.2 mL ultrapure water in the bottom residue to obtain the concentrated SHINs solution

22 After the SHINs synthesis, use TEM to determine the shell thickness of SHINs. Figure 4a shows the shape of SHINs with ~55 nm Au core and 2 nm SiO_2 shell.

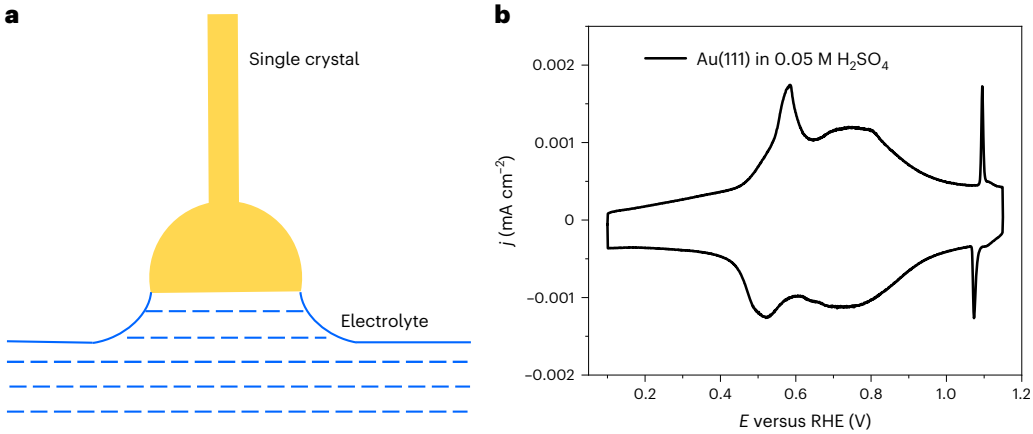

Fig. 3 | Schematic diagram and characterization of single crystals by CV. a, The hanging meniscus configuration for the experiment. **b**, The CV of Au(111) in 0.05 M H_2SO_4 with a scan rate of 10 mV s^{-1}; j and E represent the current density and potential, respectively.

PAUSE POINT The concentrated SHINs solution can be stored at room temperature in a centrifuge tube. The shelf life of SHINs can be up to a year if used for ordinary enhanced Raman experiments. In interfacial water Raman experiments, it would be better to immediately use the SHINs after preparation to avoid accumulation of impurities.

Pinhole test for the silica shell of SHINs ● Timing 15 min

23 Add 2 μL of concentrated Au@SiO_2 solution on a clean Si wafer (0.5 × 0.5 cm^2) surface and dry the wafer under an Ar stream.

24 Drop 10 μL of pyridine solution (0.01 M) on a SHINs-coated Si wafer surface. Cover it with a clean quartz coverslip.

25 Leave the coverslip like this for ~2 min to allow the pyridine molecules to adsorb onto any exposed sites on the Au surface.

26 Carry out the Raman test. If the silica shell has pinholes, it allows pyridine molecules to adsorb on the inner Au surface, and will contribute a strong Raman signal (Fig. 4b). However, if SHINs possess a pinhole-free silica shell, it will not contribute a Raman signal (Fig. 4c).

(Optional) Stability in alkaline media

▲CRITICAL It is well known that the SiO_2 shell of SHINs in acid media is very stable[51,52]. However, the SiO_2 will dissolve in alkaline media[53]. It is therefore sometimes meaningful to test their stability in a chosen solution, e.g., 1 mM NaOH.

27 Place the SHINs-coated Si wafer into a 0.01 M pyridine and 1 mM NaOH mixed solution (pH 11).

28 Collect a time series of Raman spectra. In situ Raman spectra (Fig. 4d) show that the characteristic peak of pyridine was still not discernable in 3 h. However, we observed an obvious peak at 1,010 cm^{-1} after 5 h. Therefore, SHINs can remain stable for up to 5 h.

Enhancement effect test for SHINs ● Timing 15 min

▲CRITICAL The detailed enhancement of SHINs-Au mode was calculated by pyridine as a Raman probe molecule. The corresponding formula is as follows[54–56]:

$$\mathrm{EF} = \frac{I_{\mathrm{SERS}}/N_{\mathrm{SERS}}}{I_{\mathrm{normal}}/N_{\mathrm{normal}}}$$

where I_{SERS} is the Raman peak intensity of pyridine probe molecule (the Raman peak at 1,010 cm^{-1} is selected) in enhanced spot. I_{normal} is the Raman peak intensity of pyridine solution (0.01 M). I_{SERS} and I_{normal} can be obtain experimentally. The measurement methods are as follows.

29 Collect normal Raman spectra of pyridine.
- Add 5 mL pyridine solution (0.01 M) in a small beaker
- Collect Raman signals using a confocal microscope Raman system with a 637.8 nm laser and a 50× microscope objective (0.55 numerical aperture)

  ▲CRITICAL STEP The focal point of laser must be below the liquid surface.

30 Collect SERS spectra of pyridine

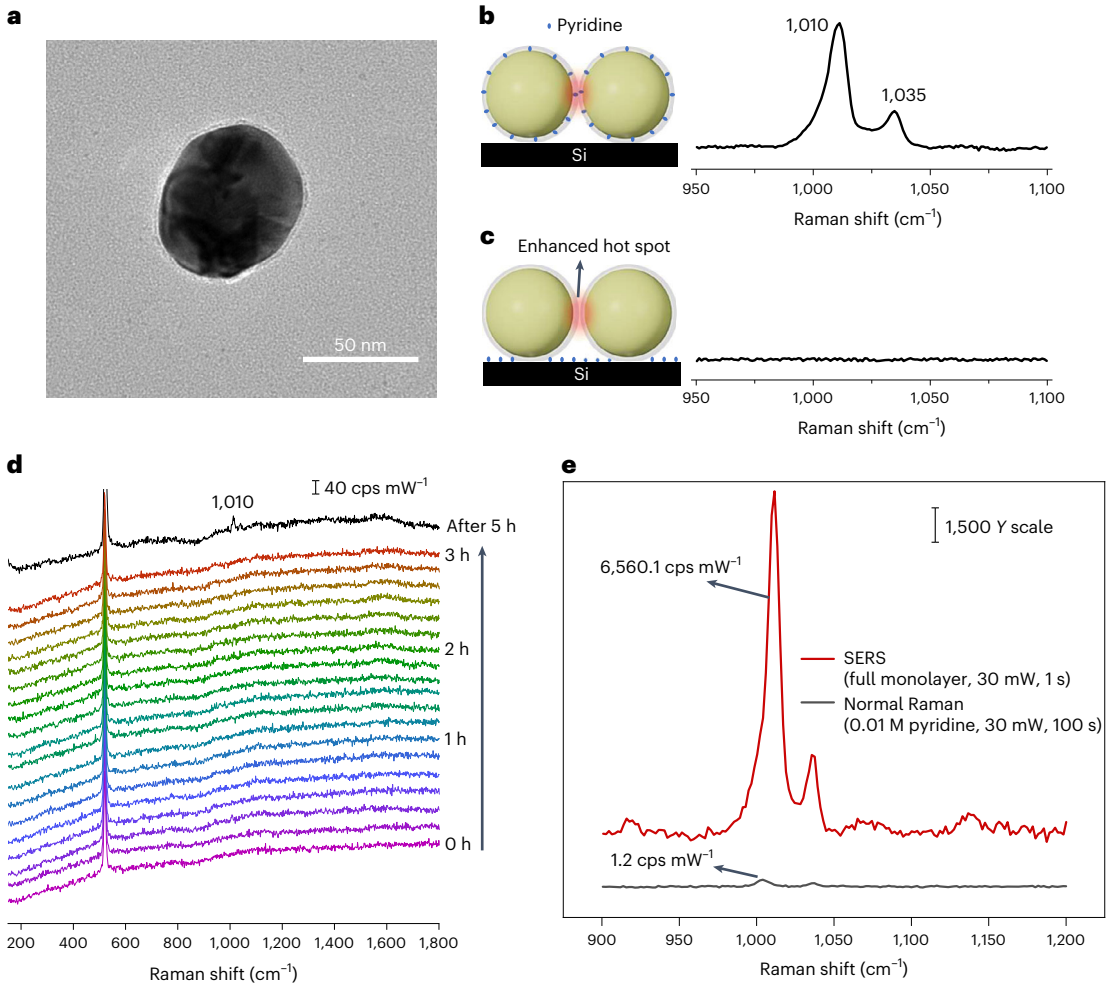

Fig. 4 | Characterization of SHINs. a, TEM image of SHINs. **b**,**c**, 55 nm Au core with 2 nm SiO_2 shell; schematic diagrams (left) and Raman spectra (right) of pinhole test using pyridine as the probe molecules on the inner Au of SHINs (**b**) and Si surface (**c**). **d**, Stability results of SHINs. In situ Raman spectra of SHINs in 0.01 M pyridine and 1 mM NaOH mixed solution (pH 11) from 1 h to 5 h. **e**, Enhancement test of SHINs. SERS spectra and normal Raman spectra of pyridine.

- Drop 2 μL of concentrated Au@SiO_2 solution (without pinholes) on a smooth Au wafer and dry the wafer under an Ar stream
- Drop 10 μL of pyridine solution (0.01 M) onto the SHINs-coated Au wafer and cover a quartz coverslip on top
- Leave for ~2 min for pyridine molecules to adsorb on the Au wafer surface
- Collect Raman signals of the SHINs-coated Au wafer under the same Raman measurement conditions with pinhole test

31 Determine the values of I_{SERS} and I_{normal} by extracting the area of Raman peaks at 1,010 cm^{-1} (SERS) and 1,003 cm^{-1} (normal) in the Raman spectra (Fig. 4e). I_{SERS} = 6,560.1 counts per second (cps) mW^{-1}, I_{normal} = 1.2 cps mW^{-1}.

? TROUBLESHOOTING

32 Calculate N_{SERS}, i.e., the number of molecules in enhanced hot spot. As a Raman probe molecule, pyridine mainly adsorbs on the smooth Au wafer surface because the inert and isolated SiO_2 shell does not adsorb molecules. Therefore, the adsorbed pyridine molecules construct a full monolayer on the Au surface.

- According to previous reports[57], the coverage (C) of pyridine on the Au surface is 3.5×10^{14} molecules cm^{-2}
- Calculate the spot diameter (d) using this formula: $d = 1.22\lambda/\mathrm{NA}$, where λ is the wavelength of laser and NA is the numerical aperture of objective

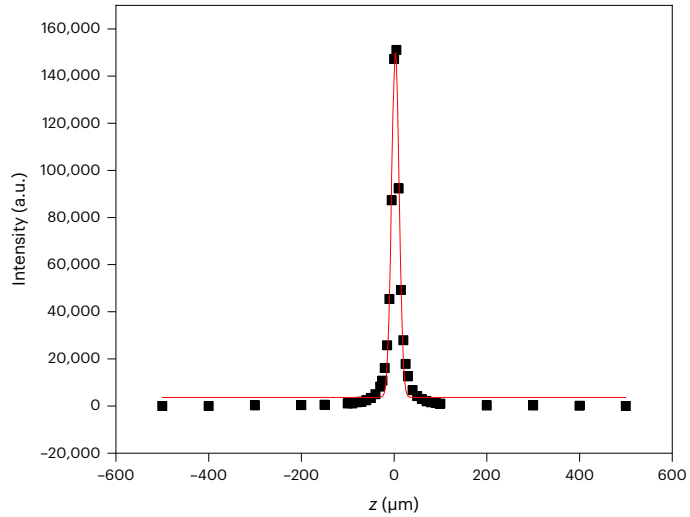

Fig. 5 | Confocal depth test of laser. Statistical intensity of Raman peak at 520.6 cm^{-1} with changing the focus depth of laser on Si(111).

- Calculate the spot area (SA) by $3.14 \times (d/2)^2$
- $N_{SERS} = SA \times C$

33 Calculate N_{normal}, i.e., the number of molecules at the Raman focal spot in the solution during normal Raman measurement.
- The calculated formula is as follows: $N_{normal} = V_{nor} \times c \times N_A$
- V_{nor} is the effective spot volume. $V_{nor} = SA \times h$, where SA is the spot area and h is the confocal depth of laser
- According to the formula of $h = \frac{\int_{-\infty}^{\infty} I(z)dz}{I_{max}}$, h can be calculated by drawing the variation curve of Raman intensity of Si wafer with the depth of focus (Fig. 5). The h is ~20.4 μm and c is the concentration of pyridine solution
- N_A is the Avogadro constant
- $N_{normal} = SA \times h \times c \times N_A$

? TROUBLESHOOTING

34 Calculate the EF from these values.
- In summary, the formula of EF can be simplified as $EF = \frac{I_{SERS}/C}{I_{normal}/(h \times c \times N_A)}$
- In our work, the EF was calculated to be 1.92×10^5 (Fig. 4e)
- The EF needs to be at least 10^5 for the collection of Raman signals of interfacial water during in situ Raman measurement. If the EF is less than 10^5, the Raman signals of bulk water might be collected rather than interfacial water

Section 3: in situ Raman

Assembly of SHINs on a single-crystal surface ● Timing 45 min

35 Wash the prepared SHINs solution (high enhancement effect and pinhole-free) three times as described in Step 21.

36 Dissolve the clean SHINs solution into 200 μL of water to make up a stock solution.

37 Drop 2 μL of SHINs stock solution onto the flamed single-crystal surface. Dry them in a gentle Ar stream to obtain SHINs single crystal.

38 Perform scanning electron microscopy (SEM) to check the distribution status of SHINs.

SHINs form a submonolayer of small, randomly distributed, two-dimensional islands, which can be seen in the SEM image in Fig. 6. The subsequent experiment can tolerate a wide range of surface coverage, but it is important to bear in mind that the presence of the SHINs decreases the physical area of the gold crystal where the electrochemical (or electrocatalytic activity) can take place. In other words, there is a trade-off between having enough SHINs to get good Raman detection and having so much that what you are detecting is no longer the reaction that you are interested in monitoring. In our experience, meaningful results can be obtained if the surface coverage is 10–25% (refs. [58,59]).

Fig. 6 | SEM image of SHINs on Au single-crystal surface. Approximately 20% coverage of SHINs on single-crystal surface.

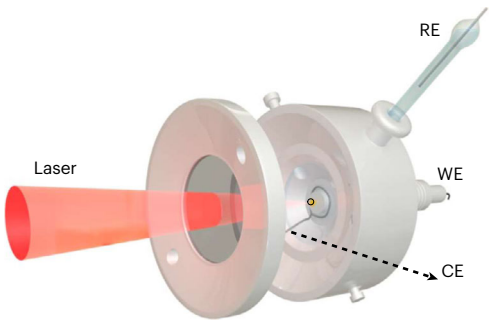

Fig. 7 | Schematic diagram of electrochemical Raman cell. WE, RE and CE represent working electrode, reference electrode and counting electrode, respectively.

Removal of impurities by HER ● Timing 30 min

▲CRITICAL Although the SHINs have been washed three times, there will still be impurities on the surface of the SHINs, especially on the single-crystal surface. The HER can be used to clean the SHINs surface to reduce the interference from impurities during Raman measurement of interfacial water.

39 Assemble the SHINs single crystal as the working electrode, the homemade RHE as the reference electrode and Pt wire as the counting electrode into a homemade Teflon Raman cell (Fig. 7). Use 0.1 M $NaClO_4$ solution as electrolyte.

40 Apply a potential of −1.3 V for 10 s to enables HER. Switch off the potential and pour out the solution quickly.

41 Perform Step 40 three more times. The clean SHINs single crystal should be used immediately.

In situ electrochemical Raman ● Timing 0.5–5 h

42 Assemble homemade Raman cell, SHINs single crystal as working electrode, RHE as reference electrode, and Pt wire as counting electrode (Fig. 7). Fill with fresh electrolyte in the Raman cell.
▲CRITICAL STEP RHE can be used directly in the Raman cell. If a non-RHE reference is used, a salt bridge is required.

43 Fix the single crystal on a Teflon thread sleeve. The distance between the single crystal and the window can be adjusted by tuning the Teflon sleeve.

44 Adjust the distance between the window and the single-crystal surface to ~50 μm by using the white light imaging system of the Raman spectrometer.
▲CRITICAL STEP 50 μm distance can effectively decrease the hydrogen bubble occurring on single-crystal surface.

45 Vertically fix the Raman cell by an iron holder to guarantee the vertical alignment of the surface of the single crystal during in situ Raman measurement. Figure 7 shows the test diagram of a vertically placed Raman cell.

46 Connect the potentiostat to electrodes of the Raman cell. Control the potentials by a potentiostat.

47 Collect the Raman signals under different potentials.

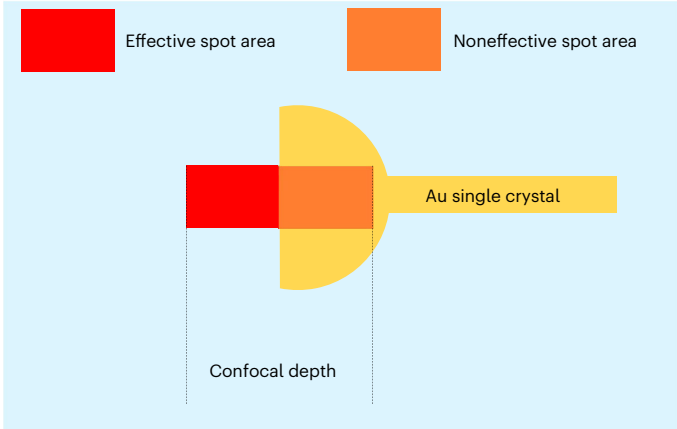

Fig. 8 | Schematic diagram of effective spot area. The confocal depth of laser (h) is 20.4 μm and half of the areas do not work when the laser focuses on the solid surface. Therefore, the effective spot area is 10.2 μm high when the laser focuses on a single-crystal surface.

Raman spectra processing ● Timing Variable; depends on the amount of data

48 Apply a potential of 1.5 V, and collect Raman spectra. While the original Raman spectrum includes all the signals of interfacial water, it also includes some of the bulk water signals. To extract the peaks related to interfacial water alone, we subtract the spectrum for bulk water alone. The Au surface will form AuO_x layers at a potential greater than 1.0 V, and the AuO_x layer can reach up to ~1.5 nm at 1.5 V (ref. [60]). The formation of AuO_x layers decreases the refractive index of the Au single crystal and increases the distance between the SHINs and the pure Au single crystal, resulting in the loss of enhancement of SHINs on an Au single-crystal surface. The inner Au of SHINs is also electrooxidized owing to the electron penetration at 1.5 V, for which the Raman signals come from bulk water. Therefore, the Raman spectrum at 1.5 V was selected as a subtracted spectral data.

49 Using the original Raman spectra, subtract the Raman spectra taken at 1.5 V; the resulting spectra are the Raman spectra of interfacial water.

While the original Raman spectrum includes all the signals of interfacial water, it also includes some of the bulk water signals. The confocal depth of laser (h) is 20.4 μm according to the previous calculation (Step 33). Thus, the effective spot area is a half column that is 10.2 μm high when the laser focuses on the single-crystal surface, as shown in Fig. 8. During the in situ electrochemical Raman test, the Raman signals come from the 10.2 μm thickness water molecules. The interfacial water molecules can be defined as within 4.0 Å distance to the single-crystal surface according to the AIMD results (details given in the following section). The proportion of interfacial water in all water molecules are calculated to be 4.0 Å/10.2 μm ≈ 3.9×10^{-5}. Raman signals of bulk water account for around half proportion, even at 1.92×10^5 high enhancement.

Section 4: AIMD simulation

Model construction

▲ **CRITICAL** The interface model is constructed on the basis of the bulk structure of the transition metals. The steps below are for the Au substrate as an example.

50 Optimize the bulk structure of Au by using Vienna ab initio simulation pack (VASP). VASP is the most widely used software for the investigation of periodic materials within the density functional theory context, and the algorithms for AIMD simulation have already been implemented in the VASP code[61].

51 Obtain the lattice parameters, with which we can construct the slab model for the simulation of Au surface.

52 Add a large vacuum space of over 15 Å in the perpendicular direction to the slab for accommodating the water molecules. We define this model as the 'Surface Model'.

53 Construct a simulation cell for water slab (without Au) under near-equilibrium conditions at room temperature. The size of the cell is the same as the Au slab in the directions parallel to the surface, while in the perpendicular direction, the size is determined according to the density of water (1 g cm^{-3}) and the number of water molecules employed in the simulation.

54 Randomly position water molecules in this simulation cell at the initial state; this can be accomplished by using Material Studio or the Visual Molecular Dynamics software.

55 Start the process of AIMD for the simulation cell to generate a more realistic model for water molecules in the liquid phase, which we can define as the 'Water Model'.
- Consider dispersion effects, for example, by utilizing the semi-empirical D3 van der Waals corrections[62]
- Set a time step of 0.5 fs or below and apply a canonical ensemble (NVT, i.e., with a fixed number of atoms, volume and temperature) via a Nose-Hoover thermostat with a target temperature of 330 K
- After ~5,000 steps, a simulation cell of water molecules under near-equilibrium conditions is generated

56 Place the 'Water Model' on top of the 'Surface Model' of Au, generating the interface model for the investigation of interfacial water.

This should be done with some care:
- First, owing to the periodic nature of the simulation cell for 'Water Model', some of the water molecules may cross the boundary of the simulation cell. These molecules would be cut if we directly implement the 'Water Model' into the vacuum space in the 'Surface Model'. Therefore, when separating the water along the boundary, we should regard each molecule as an integral unit and carefully select the periodic images of the corresponding H atoms near the boundary to avoid any broken bond
- Second, since the molecules will not establish chemical bonds with the Au surface before water splitting, the water slab and the metal slab in the interface model should be separated by 1.5–2.0 Å. Otherwise the O atoms in water would be so close to the outermost Au layer that some Au–O bonds are established, which is obviously factitious in the investigation of interfacial water

Simulation of interfacial water

▲ **CRITICAL** The parameterizations for the simulation of interfacial water are similar to that of the 'Water Model.' Owing to the large size of the supercells, only the Γ point in the Brillouin zone is employed in this simulation. The equilibrium state of the system can be evaluated by mean square displacement (MSD).

57 Conduct AIMD simulation for the interface model with at least 20,000 steps. The initial ~3 ps (6,000 steps) stage is treated as the equilibration period, and the statistical sampling should be performed in the following ~7 ps (14,000 steps).

58 Incorporate alkali (e.g., Na^+) ions into the system by placing them at the vacant space in water at a distance ~3.0–4.0 Å from the interface, and conduct AIMD simulations for these models.

▲ **CRITICAL STEP** As the simulation cell needs to be charge neutral, an equivalent number of electrons will be simultaneously introduced into the system. To avoid large abrupt forces on the water molecules, the alkali ions should be added one by one in the simulation cell after the equilibration period.

59 Calculate MSD and perform the statistical analysis of interfacial water (Fig. 9), which is a prerequisite for the calculation of electrode potential in the following steps. MSD is obtained according to the following equation:

$$\mathrm{MSD}(t) = \frac{1}{N}\sum_i \left[\mathbf{r}_i(t+t_0)\right]^2 - [\mathbf{r}(t_0)]^2,$$

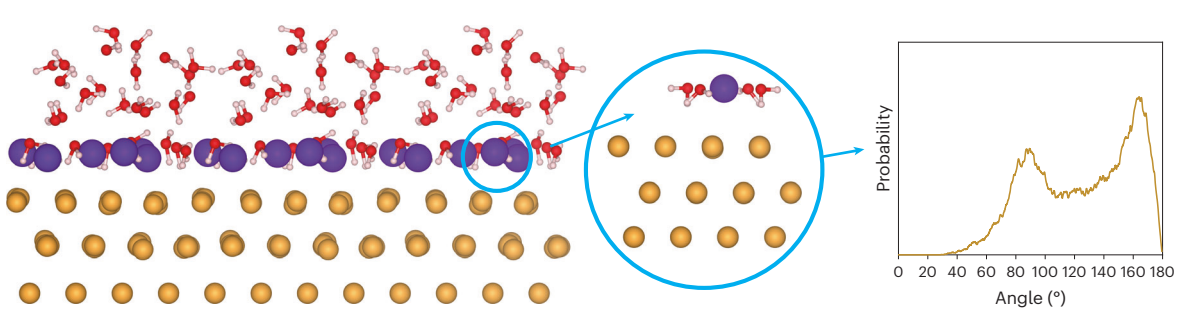

Fig. 9 | Schematic illustration of AIMD simulations for the analysis of interfacial water. Au, yellow; O, red; H, white; Na, purple. A near-equilibrium state of the interfacial model is obtained after the simulation (left), from which the local structure of water molecules around a Na^+ ion is identified (middle). Then, the statistical analysis, such as the angular distribution of water molecules, is performed for all the sampling images (right).

where $\mathbf{r}_i(t)$ is the displacement of the ith atom at time t, and N is the number of diffusing atoms in the simulation cell. A steady increase in MSD will be seen when the system is near equilibrium.

Calculation of electrode potential

▲ **CRITICAL** The calculated PZC can be directly compared with the experimental results, and therefore builds the bridge between the in situ Raman measurements and the microscopic models from AIMD simulations.

60 Calculate the PZC via the computational standard hydrogen electrode method with the following formula[63]:

$$eU^{\circ}_{\mathrm{PZC}} = -E_{\mathrm{F}}^{(i)} - e\varphi_{\mathrm{wat}}^{(i)} + \Delta_{\mathrm{DP}}A^{(w)}_{\mathrm{H_3O^+}} - \mu^{g,\circ}_{\mathrm{H^+}} - \Delta E_{\mathrm{ZP}}$$

where $E_{\mathrm{F}}^{(i)}$ is Fermi level of the system, $\varphi_{\mathrm{wat}}^{(i)}$ is the electrostatic potential of water, $\Delta_{\mathrm{DP}}A^{(w)}_{\mathrm{H_3O^+}}$ is the deprotonation free energy of a hydronium ion H_3O^+, $\mu^{g,\circ}_{\mathrm{H^+}}$ is the standard chemical potential of gas phase proton and ΔE_{ZP} is a correction for the zero-point energy of the O—H bond in hydronium ion. Only $E_{\mathrm{F}}^{(i)}$ and $\varphi_{\mathrm{wat}}^{(i)}$ are unknown and should be derived from the AIMD simulations of the interface model. $\Delta_{\mathrm{DP}}A^{(w)}_{\mathrm{H_3O^+}}$ is dependent on the composition and pseudopotentials of the simulation cells, with a value of ~15.35 eV (refs. [64,65]). $\mu^{g,\circ}_{\mathrm{H^+}}$ and ΔE_{ZP} are known constants of 15.81 eV and 0.35 eV, respectively[66,67].

61 Integrate the information from both spectroscopic characterization and atomistic simulation at a specific electrode potential. This could allow the combinatorial analysis from experiment and theory to draw a comprehensive picture of the evolution of interfacial water with respect to the electrode potential.

Statistic of interfacial water molecule

62 Extract the configurations of water molecules in the interfacial region at each corresponding electrode potential for a certain number of Na ions. The calculation results should be averaged over all the sampling images after equilibration.

63 Define the interfacial water according to the atomic density for O and H atoms in the perpendicular direction of the surface. Owing to the interaction between interfacial water and metal substrate, two density peaks will generally emerge for O and H, respectively. At negative potentials, the H atoms will be closer to the surface than O. Hence, we can use the O peak as a criterion for the definition of interfacial water. According to the simulation on Au substrate, the interfacial region is determined to be within 4.0 Å to the metal surface.

▲ **CRITICAL STEP** The above criterion is subject to the investigated system and should be exercised with caution to minimize the number of bulk water molecules mislabeled as interfacial water, as well as the number of interfacial ones mislabeled as bulk water.

64 Calculate the probability distribution of the angle (φ) between the surface normal and the bisector of the interfacial water molecules, and that (θ) between the surface normal and O–H bond direction. The φ and θ angles of the interfacial water can indicate whether the molecules are parallel to the surface or the O–H bonds tend to point towards the surface.

65 Count the number of hydrogen bonds in the interfacial region. The results could be leveraged to derive insights into the potential-dependent evolution of interfacial water configurations. The hydrogen bond can be defined by O···O distance shorter than 3.5 Å and O···O–H angle less than 35°.

66 Calculate the radial distribution function to analyze the distribution of water around Na^+ ions, which could serve as an indicator for defining the $Na{\cdot}H_2O$ cluster. Radial distribution functionis calculated as follows:

$$g(r) = \frac{1}{4\pi N\rho r^2 \Delta r}\sum_{i}^{N}\sum_{j\neq i}^{N}\delta(r - r_{ij})$$

where N is the number of O/H atoms, ρ is the corresponding average atomic density, r is the distance from the Na ion, Δr is the distance interval in the calculation and δ refers to the Dirac delta function.

It should be noted that the potential-dependent molecular orientation of water could vary for different kinds of cations in the aqueous solution. In this regard, the AIMD simulation provides the benefit of simplifying the parametrization process when compared with the force-field approach, since the latter requires ad hoc optimization of the empirically determined interatomic potentials. The easy generalization and computational efficiency of AIMD simulation makes its combination with in situ spectroscopic measurements highly promising for enriching our understanding of interfacial issues and electrocatalysis.

Troubleshooting

Troubleshooting advice can be found in Table 1.

Table 1 | Troubleshooting table

Step	Problem	Possible cause	Solution
3–5	Nonsymmetrically dispersed (111) and (100) facets Au bead	Cooling down too fast	Slow down hydrogen flame as much as possible
18, 19	Indistinct characteristic CV of Au single crystal	Electrochemical glass cell is not clean	Thoroughly and carefully clean the cell and prepare the electrolyte
20, 21	Particles agglomerate during centrifugation	Centrifuge tubes may be contaminated	Further clean centrifuge tubes before use
34	Low enhancement of SHINs	Calculation details were ignored	Double check the calculated processes
44	Difficult to control the distance between the window and the single-crystal surface	Single-crystal surface is not flat	Level the lower surface of the window, carefully adjust the electrode surface
47	Do not obtain the Raman signal of interfacial water	There are no SHINs in the collection region	The spot area is micron scale, allowing SHINs to appear within the spot area
57	Total energy does not converge to the threshold for a simulation step	The atomic configuration is unreasonable at this step	Examine the initial configuration for any broken bonds in the interfacial water region

Timing

Reagent setup: 1–3 h
Equipment setup: 10 h
Steps 1–6, preparation of Au bead: 2 h
Steps 7–13, preparation of Au half-bead single crystal: 2–3 d
Steps 14–19, characterization of Au single crystals: 1 h
Steps 20–22, preparation of Au NPs and SHINs: 2 h
Steps 23–26, pinhole test for the silica shell of SHINs: 15 min
Steps 27–28, (optional) stability in alkaline media: 5 h
Steps 29–34, enhancement effect test for SHINs: 15 min
Steps 35–38, assembly of SHINs on a single-crystal surface: 45 min
Steps 39–41, removal of the impurities by HER: 30 min
Steps 42–47, in situ electrochemical Raman: 0.5–5 h
Steps 48–49, Raman spectra processing: depends on the amount of data
Steps 50–56, model construction: 12–24 h
Steps 57–59, simulation of interfacial water: depends on the size of model and the computational sources
Steps 60–61, calculation of electrode potential: 10–30 min
Steps 62–66, statistics of interfacial water molecule: 2–5 h
These times represent averages. Specifically, some steps take more time to complete by a nonexpert in a laboratory.

Anticipated results

Figure 10 shows the spectra of both interfacial water and bulk water. The signals of interfacial water will be covered by bulk water if the enhancement effect is low. Therefore, researchers should prepare the SHINs with a high enhancement effect (EF at least 10^5) before the Raman experiment of interfacial water.

In addition, the enhancement of SHINs shows good performance when they are placed on pure Au, Ag and Cu electrodes, owing to the strong coupling effect of inner Au of SHINs with pure Au, Ag and Cu materials[68–70]. However, Cu provides only around one-sixth enhancement (1,238.3 cps mW^{-1}, Cu) compared with Au (Fig. 11a). Two obvious peaks at 528 and 613 cm^{-1} attributed to CuO_x (ref. [71]) were observed in the Raman spectra of pyridine adsorbed on Cu surface (Fig. 11b). Formation of Cu oxide on the surface in the air could reduce the coupling effect of SHINs with Cu, and further decrease

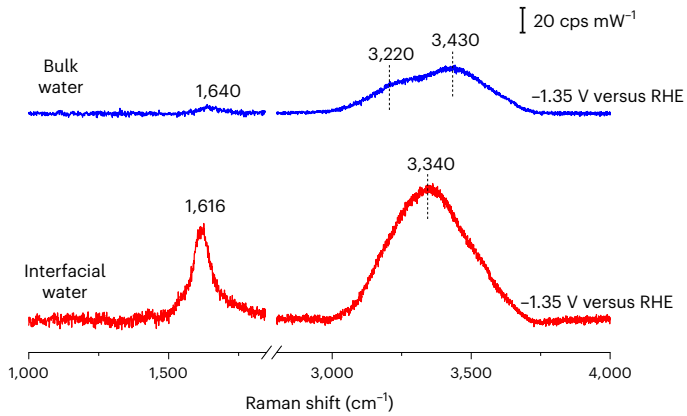

Fig. 10 | Raman spectra. Raman spectra of bulk water (blue) and interfacial water (red) at −1.35 V.

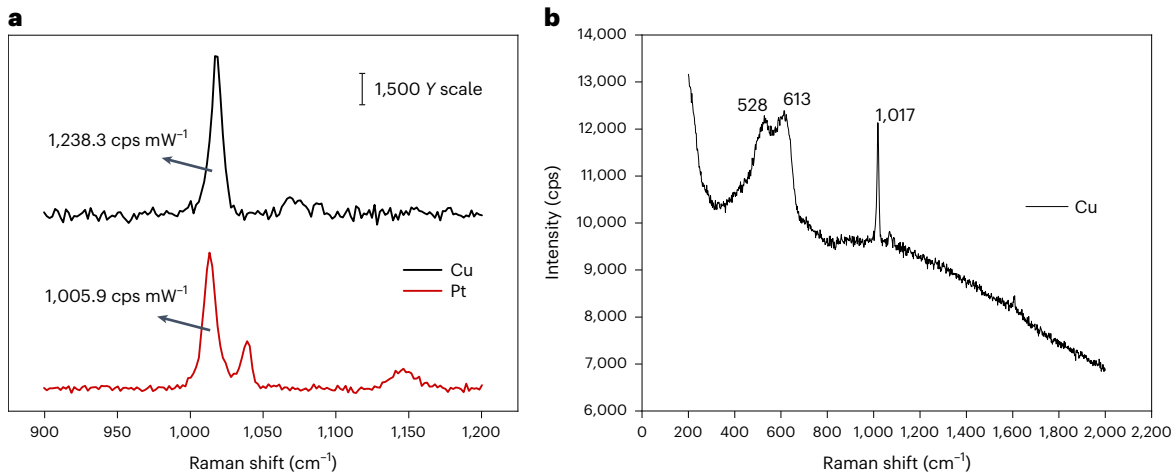

Fig. 11 | Enhancement test of SHINs. a, SERS spectra of pyridine on Cu and Pt surfaces after spectral background removal. **b**, Original SERS spectra of pyridine on Cu surface.

the enhancement. Ag is also easily oxidized in air to form a surface AgO_x layer[72]. Therefore, electrochemical reduction is required to remove the surface Cu/AgO_x layers, which will improve the enhancement of SHINs on the Cu/Ag surface, making SHINERS applicable to the study of interfacial water on Cu/Ag surfaces.

The enhancement of SHINs is much lower when adsorbed on Pt transition metal surfaces (1,005.9 cps mW^{-1}, Pt), as shown in Fig. 11a. The weak intrinsic coupling effect of SHINs with transition metal results in a weaker enhancement than is observed when Au is used. A 'borrowing strategy' that utilizes the Au and Au coupling effect by coating a transition metal on the Au surface can therefore be used to directly obtain Raman signals of interfacial water on transition metal surfaces[44].

Reporting summary

Further information on research design is available in the Nature Portfolio Reporting Summary linked to this article.

Data availability

Data generated or analyzed during this study are included in this article and ref. [44]. Source data are provided with this paper.

Code availability

The code that supports the findings of this research is available from the corresponding authors upon reasonable request.

References

1. Seh, Z. W. et al. Combining theory and experiment in electrocatalysis: insights into materials design. *Science* **355**, eaad4998 (2017).
2. Kendrick, E., Kendrick, J., Knight, K. S., Islam, M. S. & Slater, P. R. Cooperative mechanisms of fast-ion conduction in gallium-based oxides with tetrahedral moieties. *Nat. Mater.* **6**, 871–875 (2007).
3. Lim, H. et al. A universal approach for the synthesis of mesoporous gold, palladium and platinum films for applications in electrocatalysis. *Nat. Protoc.* **15**, 2980–3008 (2020).
4. Wang, X. S., Xu, C. C., Jaroniec, M., Zheng, Y. & Qiao, S. Z. Anomalous hydrogen evolution behavior in high-pH environment induced by locally generated hydronium ions. *Nat. Commun.* **10**, 1–8 (2019).
5. Mubeen, S. et al. An autonomous photosynthetic device in which all charge carriers derive from surface plasmons. *Nat. Nanotechnol.* **8**, 247–251 (2013).
6. Ye, K., Wang, G. X. & Bao, X. H. Electrodeposited Sn-based catalysts for CO_2 electroreduction. *Chin. J. Struc. Chem.* **39**, 206–213 (2020).
7. Velasco-Velez, J. J. et al. The structure of interfacial water on gold electrodes studied by x-ray absorption spectroscopy. *Science* **346**, 831–834 (2014).
8. Li, F. et al. Interplay of electrochemical and electrical effects induces structural transformations in electrocatalysts. *Nat. Catal.* **4**, 479–487 (2021).
9. Wang, H. et al. Bifunctional non-noble metal oxide nanoparticle electrocatalysts through lithium-induced conversion for overall water splitting. *Nat. Commun.* **6**, 7261 (2015).
10. Subbaraman, R. et al. Trends in activity for the water electrolyser reactions on 3*d* M(Ni,Co,Fe,Mn) hydr(oxy) oxide catalysts. *Nat. Mater.* **11**, 550–557 (2012).
11. Zhang, B. K. et al. Insights into the H_2O/V_2O_5 interface structure for optimizing water-splitting. *Chin. J. Struc. Chem.* **39**, 189–199 (2020).
12. Mesa, C. A. et al. Multihole water oxidation catalysis on haematite photoanodes revealed by operando spectroelectrochemistry and DFT. *Nat. Chem.* **12**, 82–89 (2020).
13. Wang, T. et al. Enhancing oxygen reduction electrocatalysis by tuning interfacial hydrogen bonds. *Nat. Catal.* **4**, 753–762 (2021).
14. Tian, X. et al. Engineering bunched Pt–Ni alloy nanocages for efficient oxygen reduction in practical fuel cells. *Science* **366**, 850–856 (2019).
15. Li, F. et al. Molecular tuning of CO_2-to-ethylene conversion. *Nature* **577**, 509–513 (2020).
16. Li, K. et al. Enhancement of lithium-mediated ammonia synthesis by addition of oxygen. *Science* **374**, 1593–1597 (2021).
17. Garcia de Arquer, F. P. et al. CO_2 electrolysis to multicarbon products at activities greater than 1 A cm^{-2}. *Science* **367**, 661–666 (2020).
18. Qing, G. et al. Recent advances and challenges of electrocatalytic N_2 reduction to ammonia. *Chem. Rev.* **120**, 5437–5516 (2020).
19. Vidal-Iglesias, F. J., Solla-Gullon, J., Herrero, E., Aldaz, A. & Feliu, J. M. Pd adatom decorated (100) preferentially oriented Pt nanoparticles for formic acid electrooxidation. *Angew. Chem. Int. Ed.* **49**, 6998–7001 (2010).
20. Hines, M. A. & Zare, R. N. The interaction of Co with Ni(111)—rainbows and rotational trapping. *J. Chem. Phys.* **98**, 9134–9147 (1993).
21. Marcandalli, G., Villalba, M. & Koper, M. T. M. The importance of acid–base equilibria in bicarbonate electrolytes for CO_2 electrochemical reduction and CO reoxidation studied on Au (hkl) electrodes. *Langmuir* **37**, 5707–5716 (2021).
22. Ledezma-Yanez, I. et al. Interfacial water reorganization as a pH-dependent descriptor of the hydrogen evolution rate on platinum electrodes. *Nat. Energy* **2**, 17031 (2017).
23. Zhu, S. Q., Qin, X. P., Yao, Y. & Shao, M. H. pH-dependent hydrogen and water binding energies on platinum surfaces as directly probed through surface-enhanced infrared absorption spectroscopy. *J. Am. Chem. Soc.* **142**, 8748–8754 (2020).
24. Dunwell, M., Yan, Y. & Xu, B. A surface-enhanced infrared absorption spectroscopic study of pH dependent water adsorption on Au. *Surf. Sci.* **650**, 51–56 (2016).
25. Montenegro, A. et al. Asymmetric response of interfacial water to applied electric fields. *Nature* **594**, 62–65 (2021).
26. Tong, Y., Lapointe, F., Thamer, M., Wolf, M. & Campen, R. K. Hydrophobic water probed experimentally at the gold electrode/aqueous interface. *Angew. Chem. Int. Ed.* **56**, 4211–4214 (2017).
27. Liu, W. T. & Shen, Y. R. In situ sum-frequency vibrational spectroscopy of electrochemical interfaces with surface plasmon resonance. *Proc. Natl Acad. Sci. USA* **111**, 1293–1297 (2014).
28. Ye, Y. et al. Using soft x-ray absorption spectroscopy to characterize electrode/electrolyte interfaces in-situ and operando. *J. Electron. Spectrosc. Relat. Phenom.* **221**, 2–9 (2017).
29. Nong, H. N. et al. Key role of chemistry versus bias in electrocatalytic oxygen evolution. *Nature* **587**, 408–413 (2020).
30. Blasco-Ahicart, M., Soriano-Lopez, J., Carbo, J. J., Poblet, J. M. & Galan-Mascaros, J. R. Polyoxometalate electrocatalysts based on earth-abundant metals for efficient water oxidation in acidic media. *Nat. Chem.* **10**, 24–30 (2018).

31. Nie, S. & Emory, S. R. Probing single molecules and single nanoparticles by surface-enhanced Raman scattering. *Science* **275**, 1102–1106 (1997).
32. Moskovits, M. Surface-enhanced spectroscopy. *Rev. Mod. Phys.* **57**, 783–826 (1985).
33. Liu, X. L. et al. Filter-based ultralow-frequency Raman measurement down to 2 cm^{-1} for fast Brillouin spectroscopy measurement. *Rev. Sci. Instrum.* **88**, 053110 (2017).
34. Liang, L. et al. Low-frequency shear and layer-breathing modes in Raman scattering of two-dimensional materials. *ACS Nano.* **11**, 11777–11802 (2017).
35. Fleischmann, M., Hendra, P. J., Hill, I. R. & Pemble, M. E. Enhanced Raman spectra from species formed by the coadsorption of halide ions and water molecules on silver electrodes. *J. Electroanal. Chem.* **117**, 243–255 (1981).
36. Funtikov, A. M., Sigalaev, S. K. & Kazarinov, V. E. Surface enhanced Raman scattering and local photoemission currents on the freshly prepared surface of a silver electrode. *J. Electroanal. Chem.* **228**, 197–218 (1987).
37. Chen, Y. X. & Tian, Z. Q. Dependence of surface enhanced Raman scattering of water on the hydrogen evolution reaction. *Chem. Phys. Lett.* **281**, 379–383 (1997).
38. Zou, S. Z., Chen, Y. X., Mao, B. W., Ren, B. & Tian, Z. Q. SERS studies on electrode/electrolyte interfacial water I. Ion effects in the negative potential region. *J. Electroanal. Chem.* **424**, 19–24 (1997).
39. Chen, Y. X., Zou, S. Z., Huang, K. Q. & Tian, Z. Q. SERS studies of electrode/electrolyte interfacial water part II—librations of water correlated to hydrogen evolution reaction. *J. Raman Spectrosc.* **29**, 749–756 (1998).
40. Jiang, Y. X. et al. Characterization of surface water on Au core Pt-group metal shell nanoparticles coated electrodes by surface-enhanced Raman spectroscopy. *Chem. Commun.* **28**, 4608–4610 (2007).
41. Li, J. F. et al. SERS and DFT study of water on metal cathodes of silver, gold and platinum nanoparticles. *Phys. Chem. Chem. Phys.* **12**, 2493–2502 (2010).
42. Li, J. F. et al. Shell-isolated nanoparticle-enhanced Raman spectroscopy. *Nature* **464**, 392–395 (2010).
43. Li, C. Y. et al. In situ probing electrified interfacial water structures at atomically flat surfaces. *Nat. Mater.* **18**, 697–701 (2019).
44. Wang, Y. H. et al. In situ Raman spectroscopy reveals the structure and dissociation of interfacial water. *Nature* **600**, 81–85 (2021).
45. Kohn, W. & Sham, L. J. Self-consistent equations including exchange and correlation effects. *Phys. Rev.* **140**, A1133–A1138 (1965).
46. Pham, T. A., Ping, Y. & Galli, G. Modelling heterogeneous interfaces for solar water splitting. *Nat. Mater.* **16**, 401–408 (2017).
47. Selcuk, S. & Selloni, A. Facet-dependent trapping and dynamics of excess electrons at anatase TiO_2 surfaces and aqueous interfaces. *Nat. Mater.* **15**, 1107–1112 (2016).
48. Tuckerman, M., Laasonen, K., Sprik, M. & Parrinello, M. Ab initio molecular dynamics simulation of the solvation and transport of hydronium and hydroxyl ions in water. *J. Chem. Phys.* **103**, 150–161 (1995).
49. Pham, T. A., Lee, D., Schwegler, E. & Galli, G. Interfacial effects on the band edges of functionalized si surfaces in liquid water. *J. Am. Chem. Soc.* **136**, 17071–17077 (2014).
50. Frens, G. Controlled nucleation for the regulation of the particle size in monodisperse gold suspensions. *Nat. Phys. Sci.* **241**, 20–22 (1973).
51. Wu, L., Cao, D., Huang, Y. & Li, B. G. Poly(L-lactic acid)/SiO_2 nanocomposites via in situ melt polycondensation of L-lactic acid in the presence of acidic silica sol: preparation and characterization. *Polymer* **49**, 742–748 (2008).
52. Alekseeva, M. V. et al. NiCuMo-SiO_2 catalyst for pyrolysis oil upgrading: model acidic treatment study. *Appl. Catal. A* **573**, 1–12 (2019).
53. Pekarek, R. T. et al. Intrinsic chemical reactivity of solid-electrolyte interphase components in silicon–lithium alloy anode batteries probed by FTIR spectroscopy. *J. Mater. Chem. A* **8**, 7897–7906 (2020).
54. Cai, W. B. et al. Investigation of surface-enhanced Raman scattering from platinum electrodes using a confocal Raman microscope: dependence of surface roughening pretreatment. *Surf. Sci.* **406**, 9–22 (1998).
55. Le Ru, E. C., Blackie, E., Meyer, M. & Etchegoin, P. G. Surface enhanced Raman scattering enhancement factors: a comprehensive study. *J. Phys. Chem. C.* **111**, 13794–13803 (2007).
56. Lin, H. X. et al. Uniform gold spherical particles for single-particle surface-enhanced Raman spectroscopy. *Phys. Chem. Chem. Phys.* **15**, 4130–4135 (2013).
57. Baltruschat, H., Rach, E. & Heitbaum, J. Correlation of SERS intensity potential profiles with adsorption/desorption peaks of pyridine on Au. *J. Electroanal. Chem.* **194**, 109–122 (1985).
58. Li, J. F., Rudnev, A., Fu, Y. C., Bodappa, N. & Wandlowski, T. In situ SHINERS at electrochemical single-crystal electrode/electrolyte interfaces: tuning preparation strategies and selected applications. *ACS Nano* **7**, 8940–8952 (2013).
59. Dong, J. C. et al. In situ Raman spectroscopic evidence for oxygen reduction reaction intermediates at platinum single-crystal surfaces. *Nat. Energy* **4**, 60–67 (2019).
60. Zhang, W., Bas, A. D., Ghali, E. & Choi, Y. Passive behavior of gold in sulfuric acid medium. *T. Nonferr. Metal. Soc.* **25**, 2037–2046 (2015).
61. Kresse, G. & Furthmüller, J. Efficient iterative schemes for ab initio total-energy calculations using a plane-wave basis set. *Phys. Rev. B* **54**, 11169–11186 (1996).
62. Grimme, S., Antony, J., Ehrlich, S. & Krieg, H. A consistent and accurate ab initio parametrization of density functional dispersion correction (DFT-D) for the 94 elements H-Pu. *J. Chem. Phys.* **132**, 154104 (2010).

63. Le, J., Iannuzzi, M., Cuesta, A. & Cheng, J. Determining potentials of zero charge of metal electrodes versus the standard hydrogen electrode from density-functional-theory-based molecular dynamics. *Phys. Rev. Lett.* **119**, 016801 (2017).
64. Cheng, J., Liu, X., VandeVondele, J., Sulpizi, M. & Sprik, M. Redox potentials and acidity constants from density functional theory based molecular dynamics. *Acc. Chem. Res.* **47**, 3522–3529 (2014).
65. Cheng, J. & VandeVondele, J. Calculation of electrochemical energy levels in water using the random phase approximation and a double hybrid functional. *Phys. Rev. Lett.* **116**, 086402 (2016).
66. Cheng, J., Sulpizi, M. & Sprik, M. Redox potentials and pKa for benzoquinone from density functional theory based molecular dynamics. *J. Chem. Phys.* **131**, 154504 (2009).
67. Costanzo, F., Sulpizi, M., Della Valle, R. G. & Sprik, M. The oxidation of tyrosine and tryptophan studied by a molecular dynamics normal hydrogen electrode. *J. Chem. Phys.* **134**, 244508 (2011).
68. Ding, S. Y. et al. Nanostructure-based plasmon-enhanced Raman spectroscopy for surface analysis of materials. *Nat. Rev. Mater.* **1**, 16021 (2016).
69. Ding, S. Y., You, E. M., Tian, Z. Q. & Moskovits, M. Electromagnetic theories of surface-enhanced Raman spectroscopy. *Chem. Soc. Rev.* **46**, 4042–4076 (2017).
70. Li, J. F., Zhang, Y. J., Ding, S. Y., Panneerselvam, R. & Tian, Z. Q. Core-shell nanoparticle-enhanced Raman spectroscopy. *Chem. Rev.* **117**, 5002–5069 (2017).
71. Chernyshova, I. V., Somasundaran, P. & Ponnurangam, S. On the origin of the elusive first intermediate of CO_2 electroreduction. *Proc. Natl Acad. Sci. USA* **115**, E9261–E9270 (2018).
72. Laibinis, P. E. et al. Comparison of the structures and wetting properties of self-assembled monolayers of *n*-alkanethiols on the coinage metal surfaces, copper, silver, and gold. *J. Am. Chem. Soc.* **113**, 7152–7167 (2002).

Acknowledgements

This work was financially supported by the National Key Research and Development Program of China (2019YFA0705400), the National Natural Science Foundation of China (21925404, 21991151, 21902137, 22104124, 22109003 and 22021001), the Shenzhen Fundamental Research Program (no. GXWD20201231165807007-20200807111854001), the Soft Science Research Project of Guangdong Province (2017B030301013), the '111' Project (B17027) and the State Key Laboratory of Fine Chemicals, Dalian University of Technology (KF2002). We thank the Major Science and Technology Infrastructure Project of Material Genome Big-science Facilities Platform supported by Municipal Development and Reform Commission of Shenzhen.

Author contributions

J.-F.L., Z.-Q.T. and F.P. designed the project. Y.-H.W. and S.L. conceived of and designed the protocol. Y.-H.W., Y.-J.Z. and R.-Y.Z. performed the experiments and analyzed the results. S.L., Z.-L.Y. and S.Z. performed the computations and the data analysis. Y.-H.W., J.-C.D., Y.-J.Z. and S.L. wrote the protocol. All authors discussed the results and contributed to the manuscript review.

Competing interests

The authors declare no competing interests.

Additional information

Supplementary information The online version contains supplementary material available at https://doi.org/10.1038/s41596-022-00782-8.

Correspondence and requests for materials should be addressed to Feng Pan or Jian-Feng Li.

Peer review information *Nature Protocols* thanks Alexis Grimaud and the other, anonymous, reviewer(s) for their contribution to the peer review of this work.

Received: 29 April 2022; Accepted: 12 September 2022;
Published online: 04 January 2023

Related links

Key references using this protocol

Wang, Y. H. et al. *Nature* **600**, 81–85 (2021): https://doi.org/10.1038/s41586-021-04068-z
Li, C. Y. et al. *Nat. Mater.* **18**, 697–701 (2019): https://doi.org/10.1038/s41563-019-0356-x

nature portfolio

Corresponding author(s): Jian-Feng Li

Last updated by author(s): Aug 26, 2022

Reporting Summary

Nature Portfolio wishes to improve the reproducibility of the work that we publish. This form provides structure for consistency and transparency in reporting. For further information on Nature Portfolio policies, see our Editorial Policies and the Editorial Policy Checklist.

Please do not complete any field with "not applicable" or n/a. Refer to the help text for what text to use if an item is not relevant to your study.
For final submission: please carefully check your responses for accuracy; you will not be able to make changes later.

Statistics

For all statistical analyses, confirm that the following items are present in the figure legend, table legend, main text, or Methods section.

n/a	Confirmed	
☐	☒	The exact sample size (*n*) for each experimental group/condition, given as a discrete number and unit of measurement
☐	☒	A statement on whether measurements were taken from distinct samples or whether the same sample was measured repeatedly
☐	☒	The statistical test(s) used AND whether they are one- or two-sided *Only common tests should be described solely by name; describe more complex techniques in the Methods section.*
☐	☒	A description of all covariates tested
☐	☒	A description of any assumptions or corrections, such as tests of normality and adjustment for multiple comparisons
☐	☒	A full description of the statistical parameters including central tendency (e.g. means) or other basic estimates (e.g. regression coefficient) AND variation (e.g. standard deviation) or associated estimates of uncertainty (e.g. confidence intervals)
☐	☒	For null hypothesis testing, the test statistic (e.g. *F*, *t*, *r*) with confidence intervals, effect sizes, degrees of freedom and *P* value noted *Give P values as exact values whenever suitable.*
☐	☒	For Bayesian analysis, information on the choice of priors and Markov chain Monte Carlo settings
☐	☒	For hierarchical and complex designs, identification of the appropriate level for tests and full reporting of outcomes
☐	☒	Estimates of effect sizes (e.g. Cohen's *d*, Pearson's *r*), indicating how they were calculated

Our web collection on statistics for biologists contains articles on many of the points above.

Software and code

Policy information about availability of computer code

Data collection	Labspec_6 was used to collect Raman data; CHI 760E was used to collect electrochemical data.
Data analysis	Only “Origin 2018” software was used to analyze data.

For manuscripts utilizing custom algorithms or software that are central to the research but not yet described in published literature, software must be made available to editors and reviewers. We strongly encourage code deposition in a community repository (e.g. GitHub). See the Nature Portfolio guidelines for submitting code & software for further information.

Data

Policy information about availability of data

All manuscripts must include a data availability statement. This statement should provide the following information, where applicable:

- Accession codes, unique identifiers, or web links for publicly available datasets
- A description of any restrictions on data availability
- For clinical datasets or third party data, please ensure that the statement adheres to our policy

The data generated or analyzed during this study are included in this article. Source data are provided with this paper.

Human research participants

Policy information about studies involving human research participants and Sex and Gender in Research.

Reporting on sex and gender	*Use the terms sex (biological attribute) and gender (shaped by social and cultural circumstances) carefully in order to avoid confusing both terms. Indicate if findings apply to only one sex or gender; describe whether sex and gender were considered in study design whether sex and/or gender was determined based on self-reporting or assigned and methods used. Provide in the source data disaggregated sex and gender data where this information has been collected, and consent has been obtained for sharing of individual-level data; provide overall numbers in this Reporting Summary. Please state if this information has not been collected. Report sex- and gender-based analyses where performed, justify reasons for lack of sex- and gender-based analysis.*
Population characteristics	*Describe the covariate-relevant population characteristics of the human research participants (e.g. age, genotypic information, past and current diagnosis and treatment categories). If you filled out the behavioural & social sciences study design questions and have nothing to add here, write "See above."*
Recruitment	*Describe how participants were recruited. Outline any potential self-selection bias or other biases that may be present and how these are likely to impact results.*
Ethics oversight	*Identify the organization(s) that approved the study protocol.*

Note that full information on the approval of the study protocol must also be provided in the manuscript.

Field-specific reporting

Please select the one below that is the best fit for your research. If you are not sure, read the appropriate sections before making your selection.

☐ Life sciences ☐ Behavioural & social sciences ☐ Ecological, evolutionary & environmental sciences

For a reference copy of the document with all sections, see nature.com/documents/nr-reporting-summary-flat.pdf

Life sciences study design

All studies must disclose on these points even when the disclosure is negative.

Sample size	*Describe how sample size was determined, detailing any statistical methods used to predetermine sample size OR if no sample-size calculation was performed, describe how sample sizes were chosen and provide a rationale for why these sample sizes are sufficient.*
Data exclusions	*Describe any data exclusions. If no data were excluded from the analyses, state so OR if data were excluded, describe the exclusions and the rationale behind them, indicating whether exclusion criteria were pre-established.*
Replication	*Describe the measures taken to verify the reproducibility of the experimental findings. If all attempts at replication were successful, confirm this OR if there are any findings that were not replicated or cannot be reproduced, note this and describe why.*
Randomization	*Describe how samples/organisms/participants were allocated into experimental groups. If allocation was not random, describe how covariates were controlled OR if this is not relevant to your study, explain why.*
Blinding	*Describe whether the investigators were blinded to group allocation during data collection and/or analysis. If blinding was not possible, describe why OR explain why blinding was not relevant to your study.*

Behavioural & social sciences study design

All studies must disclose on these points even when the disclosure is negative.

Study description	*Briefly describe the study type including whether data are quantitative, qualitative, or mixed-methods (e.g. qualitative cross-sectional, quantitative experimental, mixed-methods case study).*
Research sample	*State the research sample (e.g. Harvard university undergraduates, villagers in rural India) and provide relevant demographic information (e.g. age, sex) and indicate whether the sample is representative. Provide a rationale for the study sample chosen. For studies involving existing datasets, please describe the dataset and source.*
Sampling strategy	*Describe the sampling procedure (e.g. random, snowball, stratified, convenience). Describe the statistical methods that were used to predetermine sample size OR if no sample-size calculation was performed, describe how sample sizes were chosen and provide a rationale for why these sample sizes are sufficient. For qualitative data, please indicate whether data saturation was considered, and what criteria were used to decide that no further sampling was needed.*

Data collection	*Provide details about the data collection procedure, including the instruments or devices used to record the data (e.g. pen and paper, computer, eye tracker, video or audio equipment) whether anyone was present besides the participant(s) and the researcher, and whether the researcher was blind to experimental condition and/or the study hypothesis during data collection.*
Timing	*Indicate the start and stop dates of data collection. If there is a gap between collection periods, state the dates for each sample cohort.*
Data exclusions	*If no data were excluded from the analyses, state so OR if data were excluded, provide the exact number of exclusions and the rationale behind them, indicating whether exclusion criteria were pre-established.*
Non-participation	*State how many participants dropped out/declined participation and the reason(s) given OR provide response rate OR state that no participants dropped out/declined participation.*
Randomization	*If participants were not allocated into experimental groups, state so OR describe how participants were allocated to groups, and if allocation was not random, describe how covariates were controlled.*

Ecological, evolutionary & environmental sciences study design

All studies must disclose on these points even when the disclosure is negative.

Study description	*Briefly describe the study. For quantitative data include treatment factors and interactions, design structure (e.g. factorial, nested, hierarchical), nature and number of experimental units and replicates.*
Research sample	*Describe the research sample (e.g. a group of tagged Passer domesticus, all Stenocereus thurberi within Organ Pipe Cactus National Monument), and provide a rationale for the sample choice. When relevant, describe the organism taxa, source, sex, age range and any manipulations. State what population the sample is meant to represent when applicable. For studies involving existing datasets, describe the data and its source.*
Sampling strategy	*Note the sampling procedure. Describe the statistical methods that were used to predetermine sample size OR if no sample-size calculation was performed, describe how sample sizes were chosen and provide a rationale for why these sample sizes are sufficient.*
Data collection	*Describe the data collection procedure, including who recorded the data and how.*
Timing and spatial scale	*Indicate the start and stop dates of data collection, noting the frequency and periodicity of sampling and providing a rationale for these choices. If there is a gap between collection periods, state the dates for each sample cohort. Specify the spatial scale from which the data are taken*
Data exclusions	*If no data were excluded from the analyses, state so OR if data were excluded, describe the exclusions and the rationale behind them, indicating whether exclusion criteria were pre-established.*
Reproducibility	*Describe the measures taken to verify the reproducibility of experimental findings. For each experiment, note whether any attempts to repeat the experiment failed OR state that all attempts to repeat the experiment were successful.*
Randomization	*Describe how samples/organisms/participants were allocated into groups. If allocation was not random, describe how covariates were controlled. If this is not relevant to your study, explain why.*
Blinding	*Describe the extent of blinding used during data acquisition and analysis. If blinding was not possible, describe why OR explain why blinding was not relevant to your study.*

Did the study involve field work? ☐ Yes ☐ No

Field work, collection and transport

Field conditions	*Describe the study conditions for field work, providing relevant parameters (e.g. temperature, rainfall).*
Location	*State the location of the sampling or experiment, providing relevant parameters (e.g. latitude and longitude, elevation, water depth).*
Access & import/export	*Describe the efforts you have made to access habitats and to collect and import/export your samples in a responsible manner and in compliance with local, national and international laws, noting any permits that were obtained (give the name of the issuing authority, the date of issue, and any identifying information).*
Disturbance	*Describe any disturbance caused by the study and how it was minimized.*

Reporting for specific materials, systems and methods

We require information from authors about some types of materials, experimental systems and methods used in many studies. Here, indicate whether each material, system or method listed is relevant to your study. If you are not sure if a list item applies to your research, read the appropriate section before selecting a response.

Materials & experimental systems

n/a	Involved in the study
☐	☐ Antibodies
☐	☐ Eukaryotic cell lines
☐	☐ Palaeontology and archaeology
☐	☐ Animals and other organisms
☐	☐ Clinical data
☐	☐ Dual use research of concern

Methods

n/a	Involved in the study
☐	☐ ChIP-seq
☐	☐ Flow cytometry
☐	☐ MRI-based neuroimaging

Antibodies

Antibodies used	*Describe all antibodies used in the study; as applicable, provide supplier name, catalog number, clone name, and lot number.*
Validation	*Describe the validation of each primary antibody for the species and application, noting any validation statements on the manufacturer's website, relevant citations, antibody profiles in online databases, or data provided in the manuscript.*

Eukaryotic cell lines

Policy information about cell lines and Sex and Gender in Research

Cell line source(s)	*State the source of each cell line used and the sex of all primary cell lines and cells derived from human participants or vertebrate models.*
Authentication	*Describe the authentication procedures for each cell line used OR declare that none of the cell lines used were authenticated.*
Mycoplasma contamination	*Confirm that all cell lines tested negative for mycoplasma contamination OR describe the results of the testing for mycoplasma contamination OR declare that the cell lines were not tested for mycoplasma contamination.*
Commonly misidentified lines (See ICLAC register)	*Name any commonly misidentified cell lines used in the study and provide a rationale for their use.*

Palaeontology and Archaeology

Specimen provenance	*Provide provenance information for specimens and describe permits that were obtained for the work (including the name of the issuing authority, the date of issue, and any identifying information). Permits should encompass collection and, where applicable, export.*
Specimen deposition	*Indicate where the specimens have been deposited to permit free access by other researchers.*
Dating methods	*If new dates are provided, describe how they were obtained (e.g. collection, storage, sample pretreatment and measurement), where they were obtained (i.e. lab name), the calibration program and the protocol for quality assurance OR state that no new dates are provided.*

☐ Tick this box to confirm that the raw and calibrated dates are available in the paper or in Supplementary Information.

Ethics oversight	*Identify the organization(s) that approved or provided guidance on the study protocol, OR state that no ethical approval or guidance was required and explain why not.*

Note that full information on the approval of the study protocol must also be provided in the manuscript.

Animals and other research organisms

Policy information about studies involving animals; ARRIVE guidelines recommended for reporting animal research, and Sex and Gender in Research

Laboratory animals	*For laboratory animals, report species, strain and age OR state that the study did not involve laboratory animals.*

Wild animals	*Provide details on animals observed in or captured in the field; report species and age where possible. Describe how animals were caught and transported and what happened to captive animals after the study (if killed, explain why and describe method; if released, say where and when) OR state that the study did not involve wild animals.*
Reporting on sex	*Indicate if findings apply to only one sex; describe whether sex was considered in study design, methods used for assigning sex. Provide data disaggregated for sex where this information has been collected in the source data as appropriate; provide overall numbers in this Reporting Summary. Please state if this information has not been collected. Report sex-based analyses where performed, justify reasons for lack of sex-based analysis.*
Field-collected samples	*For laboratory work with field-collected samples, describe all relevant parameters such as housing, maintenance, temperature, photoperiod and end-of-experiment protocol OR state that the study did not involve samples collected from the field.*
Ethics oversight	*Identify the organization(s) that approved or provided guidance on the study protocol, OR state that no ethical approval or guidance was required and explain why not.*

Note that full information on the approval of the study protocol must also be provided in the manuscript.

Clinical data

Policy information about clinical studies

All manuscripts should comply with the ICMJE guidelines for publication of clinical research and a completed CONSORT checklist must be included with all submissions.

Clinical trial registration	*Provide the trial registration number from ClinicalTrials.gov or an equivalent agency.*
Study protocol	*Note where the full trial protocol can be accessed OR if not available, explain why.*
Data collection	*Describe the settings and locales of data collection, noting the time periods of recruitment and data collection.*
Outcomes	*Describe how you pre-defined primary and secondary outcome measures and how you assessed these measures.*

Dual use research of concern

Policy information about dual use research of concern

Hazards

Could the accidental, deliberate or reckless misuse of agents or technologies generated in the work, or the application of information presented in the manuscript, pose a threat to:

No	Yes	
☐	☐	Public health
☐	☐	National security
☐	☐	Crops and/or livestock
☐	☐	Ecosystems
☐	☐	Any other significant area

Experiments of concern

Does the work involve any of these experiments of concern:

No	Yes	
☐	☐	Demonstrate how to render a vaccine ineffective
☐	☐	Confer resistance to therapeutically useful antibiotics or antiviral agents
☐	☐	Enhance the virulence of a pathogen or render a nonpathogen virulent
☐	☐	Increase transmissibility of a pathogen
☐	☐	Alter the host range of a pathogen
☐	☐	Enable evasion of diagnostic/detection modalities
☐	☐	Enable the weaponization of a biological agent or toxin
☐	☐	Any other potentially harmful combination of experiments and agents

ChIP-seq

Data deposition

☐ Confirm that both raw and final processed data have been deposited in a public database such as GEO.

☐ Confirm that you have deposited or provided access to graph files (e.g. BED files) for the called peaks.

Data access links *May remain private before publication.*	*For "Initial submission" or "Revised version" documents, provide reviewer access links. For your "Final submission" document, provide a link to the deposited data.*
Files in database submission	*Provide a list of all files available in the database submission.*
Genome browser session (e.g. UCSC)	*Provide a link to an anonymized genome browser session for "Initial submission" and "Revised version" documents only, to enable peer review. Write "no longer applicable" for "Final submission" documents.*

Methodology

Replicates	*Describe the experimental replicates, specifying number, type and replicate agreement.*
Sequencing depth	*Describe the sequencing depth for each experiment, providing the total number of reads, uniquely mapped reads, length of reads and whether they were paired- or single-end.*
Antibodies	*Describe the antibodies used for the ChIP-seq experiments; as applicable, provide supplier name, catalog number, clone name, and lot number.*
Peak calling parameters	*Specify the command line program and parameters used for read mapping and peak calling, including the ChIP, control and index files used.*
Data quality	*Describe the methods used to ensure data quality in full detail, including how many peaks are at FDR 5% and above 5-fold enrichment.*
Software	*Describe the software used to collect and analyze the ChIP-seq data. For custom code that has been deposited into a community repository, provide accession details.*

Flow Cytometry

Plots

Confirm that:

☐ The axis labels state the marker and fluorochrome used (e.g. CD4-FITC).

☐ The axis scales are clearly visible. Include numbers along axes only for bottom left plot of group (a 'group' is an analysis of identical markers).

☐ All plots are contour plots with outliers or pseudocolor plots.

☐ A numerical value for number of cells or percentage (with statistics) is provided.

Methodology

Sample preparation	*Describe the sample preparation, detailing the biological source of the cells and any tissue processing steps used.*
Instrument	*Identify the instrument used for data collection, specifying make and model number.*
Software	*Describe the software used to collect and analyze the flow cytometry data. For custom code that has been deposited into a community repository, provide accession details.*
Cell population abundance	*Describe the abundance of the relevant cell populations within post-sort fractions, providing details on the purity of the samples and how it was determined.*
Gating strategy	*Describe the gating strategy used for all relevant experiments, specifying the preliminary FSC/SSC gates of the starting cell population, indicating where boundaries between "positive" and "negative" staining cell populations are defined.*

☐ Tick this box to confirm that a figure exemplifying the gating strategy is provided in the Supplementary Information.

Magnetic resonance imaging

Experimental design

Design type	*Indicate task or resting state; event-related or block design.*

Design specifications	*Specify the number of blocks, trials or experimental units per session and/or subject, and specify the length of each trial or block (if trials are blocked) and interval between trials.*
Behavioral performance measures	*State number and/or type of variables recorded (e.g. correct button press, response time) and what statistics were used to establish that the subjects were performing the task as expected (e.g. mean, range, and/or standard deviation across subjects).*

Acquisition

Imaging type(s)	*Specify: functional, structural, diffusion, perfusion.*
Field strength	*Specify in Tesla*
Sequence & imaging parameters	*Specify the pulse sequence type (gradient echo, spin echo, etc.), imaging type (EPI, spiral, etc.), field of view, matrix size, slice thickness, orientation and TE/TR/flip angle.*
Area of acquisition	*State whether a whole brain scan was used OR define the area of acquisition, describing how the region was determined.*

Diffusion MRI ☐ Used ☐ Not used

Preprocessing

Preprocessing software	*Provide detail on software version and revision number and on specific parameters (model/functions, brain extraction, segmentation, smoothing kernel size, etc.).*
Normalization	*If data were normalized/standardized, describe the approach(es): specify linear or non-linear and define image types used for transformation OR indicate that data were not normalized and explain rationale for lack of normalization.*
Normalization template	*Describe the template used for normalization/transformation, specifying subject space or group standardized space (e.g. original Talairach, MNI305, ICBM152) OR indicate that the data were not normalized.*
Noise and artifact removal	*Describe your procedure(s) for artifact and structured noise removal, specifying motion parameters, tissue signals and physiological signals (heart rate, respiration).*
Volume censoring	*Define your software and/or method and criteria for volume censoring, and state the extent of such censoring.*

Statistical modeling & inference

Model type and settings	*Specify type (mass univariate, multivariate, RSA, predictive, etc.) and describe essential details of the model at the first and second levels (e.g. fixed, random or mixed effects; drift or auto-correlation).*
Effect(s) tested	*Define precise effect in terms of the task or stimulus conditions instead of psychological concepts and indicate whether ANOVA or factorial designs were used.*

Specify type of analysis: ☐ Whole brain ☐ ROI-based ☐ Both

Statistic type for inference (See Eklund et al. 2016)	*Specify voxel-wise or cluster-wise and report all relevant parameters for cluster-wise methods.*
Correction	*Describe the type of correction and how it is obtained for multiple comparisons (e.g. FWE, FDR, permutation or Monte Carlo).*

Models & analysis

n/a	Involved in the study
☐	☐ Functional and/or effective connectivity
☐	☐ Graph analysis
☐	☐ Multivariate modeling or predictive analysis

Functional and/or effective connectivity	*Report the measures of dependence used and the model details (e.g. Pearson correlation, partial correlation, mutual information).*
Graph analysis	*Report the dependent variable and connectivity measure, specifying weighted graph or binarized graph, subject- or group-level, and the global and/or node summaries used (e.g. clustering coefficient, efficiency, etc.).*
Multivariate modeling and predictive analysis	*Specify independent variables, features extraction and dimension reduction, model, training and evaluation metrics.*